

A mid-IR Plasmonic Graphene Nanorectenna-based Energy Harvester to Power IoT Sensors

Giovanni D'Arrigo¹, Rocco Citroni², Patrizia Livreri¹

¹Dept. of Engineering, University of Palermo, Palermo, Italy

²Dept. of Electronics Engineering, University of Rome Tor Vergata, Italy

Corresponding author: patrizia.livreri@unipa.it

Abstract— In this paper, the design of a graphene arrowbowtie nanoantenna mid-IR energy-harvester to power IOT wireless sensor is presented. For the first time, a sensitivity analysis of the mid-IR nanoantenna resonant frequencies in terms of different graphene number of sheets and chemical potential (μ_{cp}) without substrate and on a two-layer substrate composed of SiO₂ and Si, is carried out. The obtained simulation results by 3D CST 2020 are useful to design an efficient infrared nanorectenna, composed of the nanoantenna and a rectifying MIM diode inside the gap. The analysis of the complete energy-harvester (EH), composed of an NxM nanorectenna array, a low-pass filter, and a DC-DC converter, is reported. With an output voltage value of 3.3 V, an output current of 10 mA, and an area of about 11,57 mm², the proposed 1964x65467 nanorectenna array-based infrared energy harvester array represents an optimal solution to powering IoT wireless sensors.

Keywords— Nanoantenna, arrow bowtie, plasmonic, energy harvesting, IoT.

I. INTRODUCTION

The radiation emitted from Earth's surface is mainly centered in the middle wavelength infrared (MWIR), with its peak centered at wavelengths approximately around 10 μm (28.3 THz). New devices, called nano-rectennas, composed of nanoantennas and rectifying diode, capable of converting the electromagnetic radiation into current, and serving as power supply to power wireless battery-free IOT sensors are being developed. Graphene, formed of carbon atoms arranged in a two-dimensional hexagonal structure with unique electronic, optical, and mechanical properties, is becoming increasingly more attractive due to its plasmonic properties. Plasmons are collective electron oscillations usually excited at metal surfaces by a light source. This plasmonic effect occurs at the GHz-THz range and is fundamental for energy harvesting applications [1-19]. In this work, the design for a 28.3 THz energy harvesting graphene nanoantenna for powering IOT sensors is presented. The paper is organized as follows. In section II, the simulations of an arrow nanoantenna and the sensitivity analysis without and on a substrate are carried out by 2020 CST Studio. In section III, the design of the infrared nanorectenna, composed of the nanoantenna designed in section 2 and a rectifying MIM diode is carried out. Finally, in section IV the analysis of the 49498x14286 nanoarray infrared Energy Harvester is reported.

II. ARROW NANOANTENNAS DESIGN: SIMULATION AND SENSITIVITY ANALYSIS

An arrow nanoantenna, shaped as two opposite arrowheads separated by a gap, with an enhanced electromagnetic field in the gap, is considered as geometry [20-23]. In Fig. 1, the CST schematic model of the simulated arrow bowtie nanoantenna is shown. A cut is made at the angle in the gap, to enhance the electromagnetic field in the gap and to reduce the nanoantennas impedance, necessary condition to have an optimal matching between the nanoantenna and rectifying diode. Moreover, with the cut a decreasing in the resonant frequencies does occur.

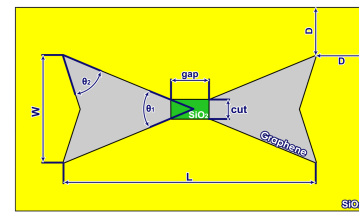


Fig. 1. Schematic Model of the arrow bowtie nanoantenna.

The nanoantenna has been simulated, at first, without substrate and, finally, on a two-layer substrate, composed of silicon oxide and high conductivity silicon, as shown in Fig. 2.

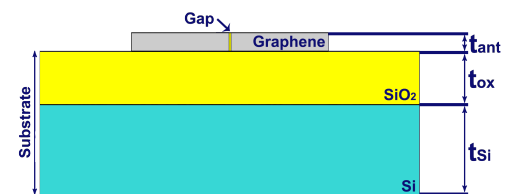


Fig. 2. Model of the nanoantenna and 2-layer substrate (sideview).

An optimization of the nanoantenna geometries in terms of width, length, cut, thickness, and angles, is carried out by CST Studio 2020, in order to obtain a surface plasmonic of nanoantennas resonant frequency in the middle infrared range, at about 28.3 THz [24]. In Table I, the optimized design simulation values in terms of geometric dimensions (gap, cut, and width) are reported. The values of the angles, optimized in

TABLE I
ARROW NANOANTENNAS GEOMETRIC DIMENSIONS

θ_1	θ_2	Cut [nm]	Gap [nm]	L [nm]	W [nm]
45°	50°	10	3	300	133

terms of the field enhancement, come from previously simulations [25].

In Fig. 3, the real and imaginary part of the simulated arrow nanoantenna impedance without the substrate is shown, for two different values of the cut (10 nm green curves, 20 nm red curves).

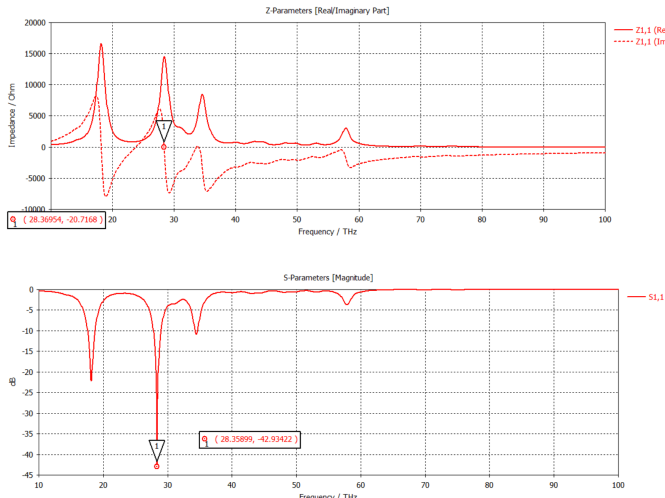


Fig. 3. Real and Imaginary part of the impedance for an arrow nanoantenna without substrate with geometric dimensions given in Table I (a) S11 parameter (b).

For the first time, a sensitivity analysis in terms of graphene thickness (sheets) and chemical potential (μ_{cp}), is carried out. The simulation results of the sensitivity analysis are reported in Table II.

The thickness of the graphene is related to its layered characteristic form, according to Eq. 1:

$$t = 0.335 \cdot N + 0.14 \cdot (N - 1) \quad (1)$$

where t is the total graphene thickness expressed in nm, and N is the number of graphene sheets. The single layer graphene thickness is equal to 0.335 nm, or 0.14 nm if the space organization of the carbon atom bonds is taken into account. In Fig. 4, the gap voltage of the nanoantenna vs frequency is plotted.

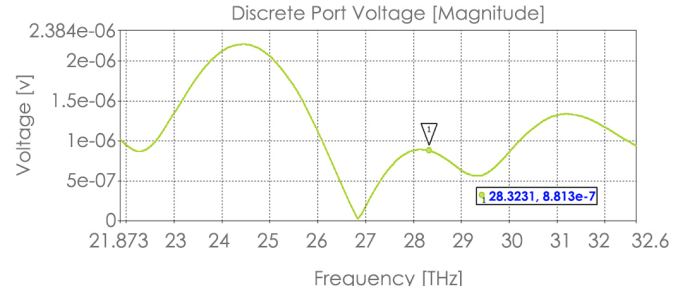


Fig. 4. Gap voltage vs frequency.

TABLE II
NANOANTENNA AND SUBSTRATE LAYER THICKNESS

t_{ant} [nm]	Graphene sheets	t_{ox} [nm]	t_{Si} [nm]	μ_{cp} [eV]
71.585	151	300	500	0.3

The resonant frequency vs the number of the sheets, has been simulated and the result showing a decreasing low has been plotted in Fig. 5. The resonant frequency vs the graphene electro-chemical potential, is plotted in Fig. 6. By using a higher chemical potential [26-28], fewer sheets are used to tune the nanoantenna in the desired range. By approximately doubling the total length of the nanoantenna, there is a more pronounced zero crossing and the real part of the impedance is lower by an order of magnitude. Finally, in Fig. 7, the optimized real and imaginary part of the nanoantenna impedance, obtained by varying the geometric parameters, the graphene sheets and chemical potential, with a resonance frequency equal to 28.29 THz is shown. Silicon oxide is inserted in the gap between the two arrowheads to simulate the nanoantenna in real conditions with the rectifying MIM diode.

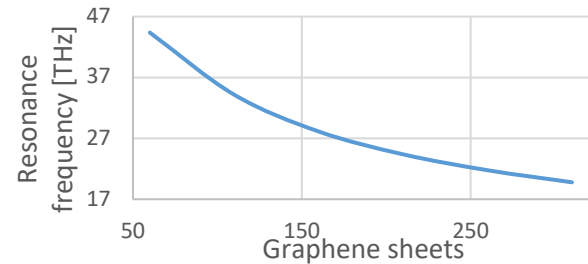


Fig. 5. Nanoantenna resonant frequency vs graphene sheets.

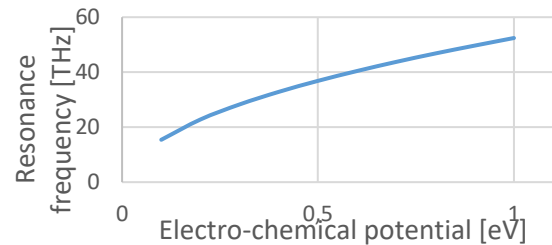


Fig. 6. Resonant frequency vs electro-chemical potential.

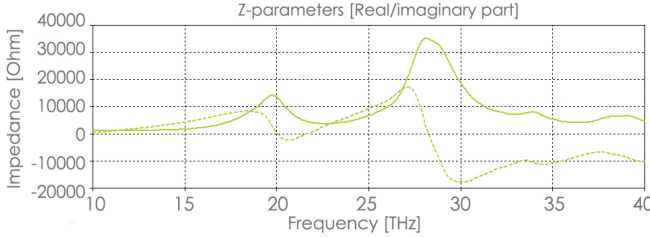


Fig. 7. Real and Imaginary part of the nanoantenna impedance with 2-layer substrate.

III. THE NANODIODE RECTIFIER

The nanoantenna represents only a passive device unable to convert the high frequency signal harvested directly in DC power [29]. Therefore, an ultra-high speed diode able to rectify THz frequencies is mandatory. Today, the best choose is represented by diodes composed of a single insulator sandwiched between different metals known as metal insulator metal (MIM). These devices have to respect many requirements imposed for THz frequency rectification, like asymmetry, (Asym), nonlinearity (NL), and responsivity (S), which represent the figure of merits (FOMs). In addition, small size, small turn on voltage (TOV), reverse-bias leakage around $1\mu\text{A}$ or less, lower RC time constant (needed to obtain high cut-off frequency and to allow a correct THz rectification) and coupling efficiency between the resistance of the diode and the resistance of the nanoantenna (needed to obtain the maximum power transfer to the load) are open questions. To obtain a more efficient rectification process a MIM diode must have simultaneously high FOMs and a low resistance. Unfortunately, not all of these criteria can be obtained with a single insulator layer. Today, the scientific community has made significant progress in the field of MIM diodes. Multiple insulators layers sandwiched between two similar or dissimilar metal electrodes constitute a technology premised able to overcome the issues exposed above. This device is known as MIⁿM, where n represents the number of ultra-thin insulator layers. When n=2, the structure is known as metal-insulator-insulator-metal (MIIM). Recent studies indicate that the best result was obtained in [30], by considering a graphene/hexagonal boron nitride (h-BN)/graphene heterostructure (Gr-h-BN-Gr). This structure, printed on a Si/SiO₂ substrate with 90 nm thermal SiO₂, consists of graphene as contacts and hexagonal boron nitride (h-BN) as insulator with a thickness less than 6 nm. The results obtained in terms of FOMs indicate an Asym of 1000, an NL of 40, a zero-bias S of 2.75 V^{-1} , a peak S of 12 V^{-1} , and a current density J_{ON} of 0.02 A/cm^2 for a bias of 1 V. However, this device is not the best candidate due to high voltage bias, which makes it inadequate for energy harvesting applications.

IV. THE NANORECTENNA SYSTEM

The rectenna system includes a nanoantenna and a rectifying diode inserted in the gap of the nanoantenna to convert high frequency electromagnetic fields into direct current. In Fig. 8,

the equivalent circuit of the rectenna system is shown. The nanoantenna is represented as a voltage generator V_{open} and an impedance Z_A . The rectifying diode can be represented by a junction capacitance C_D , as the switching time of the diode, and a non-linear resistor R_D .

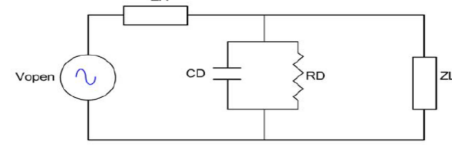


Fig. 8. Equivalent circuit of rectenna system.

For the simulation of the infrared energy harvesting system, a M-I-M diode and an LTC3108 DC-DC converter from Analog Devices have been used as rectifier diodes. As first step, a nanoantenna value $V_{open} = 1.6 \text{ mV}$ was obtained by CST studio simulation, and a value of $Z_A = 3.4 \text{ k}\Omega$ was obtained corresponding to the resonant frequency $f = 28.3 \text{ THz}$.

Metal insulator metal diodes, which may be used up to 30 THz, must show adequate figure of merits (FOMs) as asymmetry, (Asym) nonlinearity (NL) and responsivity (S) around zero bias and cut-off frequency [29]. The thickness of the oxide layer is 15 nm, whereas the thickness of the metal is around 100 nm. For the calculation of the impedance matching, the diode capacity C_D can be neglected as it behaves like a low pass filter. The current through the circuit can be given by Eq. 3:

$$I = \frac{V_{open}}{R_A + \frac{R_D R_L}{R_D + R_L}} \quad (3)$$

The condition for the best impedance matching is obtained for R_D greater than R_A and R_L with $R_A = R_L$. We must also consider the impedance matching with the step-up dc-dc converter, Z_{BOOST} . For a good matching, the rectenna array system must have an impedance value equal to Z_{BOOST} , which in the case of LTC3108 is equal to 3Ω . The equivalent resistance of each single rectenna is given by Eq. 4:

$$R_{RECT} = \frac{R_A R_D}{R_A + R_D} = 96\Omega \quad (4)$$

with $R_A = 3.4 \text{ k}\Omega$ and $R_D = 100 \Omega$ in the case of M-I-M diodes. To obtain a good impedance matching with the step-up dc-dc converter we build an $N \times M$ array of rectennas with $R_{eq.array}$ equal to Z_{BOOST} and given by Eq. 5:

$$R_{eq.array} = \frac{N}{M} R_{RECT} = \frac{N}{M} \frac{R_A R_D}{R_A + R_D} \quad (5)$$

From (5), with $Z_{BOOST} = 3 \Omega$, and for $R_{eq.array}$ equal to Z_{BOOST} , Eq. 6 occurs:

$$\frac{N}{M} = R_{eq.array} * \frac{R_A + R_D}{R_A R_D} = 0.03 \quad (6)$$

For the choice of N and M two considerations occur, the first is that N depends on the output voltage to be supplied to the boost, whereas, the second, that M depends on the input resistance of

the boost. To achieve good matching between the rectenna system and the harvester, the rectenna output voltage must be greater than the lowest acceptable input voltage from the boost. This gives us a lower bound for the choice of N. The input voltage of LTC3108 can vary from 20 mV to 500 mV, therefore the minimum and maximum value of the output voltage from the array are 40 mV to 1 V, equal to 2 V_{BOOST}.

Finally, N is given by Eq. 7:

$$N = \frac{V_{o, \text{array}}}{V_{DC}} = \frac{2V_{I\text{boost}}}{\frac{V_{open}}{\pi}} \quad (7)$$

By choosing the V_{BOOST} maximum equal to 500 mV and the V_{DC} value obtained by dividing the V_{OPEN} to π (corresponding to a rectified half wave), the following values of N and M were obtained: N=1964 and M=65467.

The area occupied by the array is given by Eq. 8:

$$A_{\text{array}} = N * M * A_{\text{rectenna}} = 11,57 \text{ mm}^2 \quad (8)$$

The equivalent circuit at the input of the step-up DC-DC converter is shown in Figure 9.

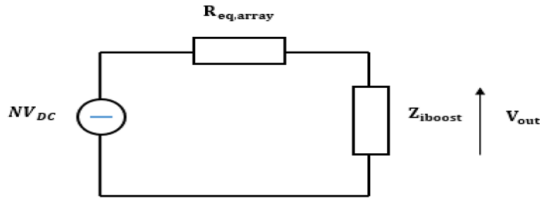


Fig. 9. Equivalent circuit for the boost input.

The complete system was simulated using the LT spice simulation program. The output voltage obtained is equal to V_{out} = 3.3V, which makes it suitable to power IoT wireless sensors, as shown in Fig. 10 [31].

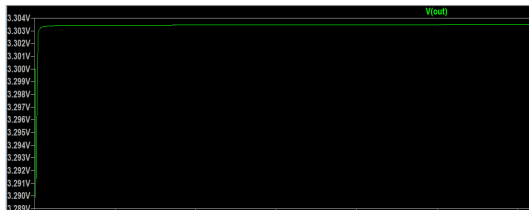


Fig. 10. Boost output voltage.

V. CONCLUSIONS

The design of a complete infrared energy-harvester (EH), composed of an NxM nanorectenna array with graphene nanoantenna and MIM diode, a low-pass filter, and a DC-DC converter, is reported. With an output voltage value of 3.3 V, an output current of 10 mA, and an area of about 11,57 mm², the proposed 1964x65467 nanorectenna array-based infrared energy harvester represents an optimal solution to power IoT wireless sensors.

REFERENCES

- [1] Koppens, F. H.; Chang, D. E.; García De Abajo, F. J. (2011) "Graphene plasmonics: A platform for strong light-matter interactions".
- [2] Yan, Hugen; Low, Tony; Zhu, Wenjuan; Wu, Yanqing; Freitag, Marcus; Li, Xuesong; Guinea, Francisco; Avouris, Phaedon; Xia, Fengnian (2013) "Damping pathways of mid-infrared plasmons in graphene nanostructures", Nature Photonics.
- [3] L A Falkovsky 2008 J. Phys.: Conf. Ser. 129 012004.
- [4] Anqi Yu, "Tunable strong THz absorption assisted by graphene-dielectric stacking structure", Superlattices and Microstructures, Volume 122, 2018, Pages 461-470, ISSN 0749-6036, <https://doi.org/10.1016/j.spmi.2018.06.065>.
- [5] Cai W., Shalaev V., Optical Metamaterials Fundamentals and Applications, Springer 2010.
- [6] Gadalla, M. N., Abdel-Rahman, M. & Shamim, A. Design, optimization and fabrication of a 28.3 thz nano-rectenna for infrared detection and rectification. Scientific Reports 4, 4270 (2014).
- [7] Chekini, A.; Sheikhaei, S.; Neshat, M. A Novel Plasmonic Nanoantenna Structure for Solar Energy Harvesting, 2016 Fourth International Conference on Millimeter-Wave and Terahertz Technologies (MMWaTT), Tehran, 2016, pp. 20-24.
- [8] Vandebosch, Guy A.E.; Zhongkun, M.A. Upper bounds for the solar energy harvesting efficiency of nano-antennas, Nano Energy (2012) 1, 494-502.
- [9] Alù, A.; Engheta, N. Input Impedance, Nanocircuit Loading, and Radiation Tuning of Optical Nanoantennas, Phys. Rev. Lett. 101, 043901 (2008), pp.1-4.
- [10] Maksymov I. S., Davoyan A. R., Simovski, C. Belov P., Kivshar Yu. S., Multifrequency broadband tapered plasmonic nanoantennas, May 2011, Optics Communications 285(5), pp.1-5.
- [11] Maksymov I. S., Staude I., Miroshnichenko A. E. and Kivshar Y. S. Optical Yagi-Uda nanoantennas, Nanophotonics 1 (2012), pp. 65-81
- [12] Krasnok A.E., Maksymov I. S., Denisyuk A. I., Belov P. A., Miroshnichenko A. E., Simovski C. R., Kivshar Y. S., Optical nanoantennas, Physics, Uspekhi 56 (6), pp. 539-564 (2013).
- [13] Xu, Y.; Tucker, E.; Boreman, G.; Raschke, M.B.; Lail, B.A. Optical nanoantenna input impedance, ACS Photonics, 3, 5, 881-885, 2016.
- [14] El-Toukhy, Y.M.; Hussein, M.; Hameed, M.F.O.; Heikal, A.M.; Abd-Elrazzak, M.M.; Obaya, S.S.A. Optimized tapered dipole nanoantenna as efficient energy harvester, Optics Express, 24, 14, A1107-A1122, 2016.
- [15] Ma, Z.; Vandebosch, G.A.E. Optimal solar energy harvesting efficiency of nano-rectenna systems, Solar Energy, 88, 163-174, 2013.
- [16] Javier Gonzalez F., Ilic B., Alda J., and Boreman G.D., Antenna-Coupled Infrared Detectors for Imaging Applications, in IEEE Journal of Selected Topics in Quantum Electronics, vol. 11, no. 1, pp. 117-120, Jan.-Feb. 2005.

- [17] Ma Z, Vandenbosch G.A. Input impedance of optical metallic nanodipole over 300 nm – 1200 nm wavelength, IEEE 7th European Conference on Antennas and Propagation (EuCAP), 2013.
- [18] Yana, S.; Tumendemberela, B.; Zhenga, X.; Vladimir Volskiya, V.; Vandenbosch, G.A.E.; Moshchalkova, V.V. Optimizing the bowtie nano-rectenna topology for solar energy harvesting applications, *Solar Energy* 157 (2017) 259–262.
- [19] Lin L., Zheng Y., Optimizing plasmonic nanoantennas via coordinated multiple coupling, *Scientific Reports* volume 5, Article number: 14788 (2015), pp.1-11.
- [20] P. Livreri, G. Raimondi, "A Novel Plasmonic Nanoantenna for High Efficiency Energy Harvesting Applications", 2020 IEEE 20th Mediterranean Electrotechnical Conference (MELECON) , 2020, pp. 193-196, doi: 10.1109/MELECON48756.2020.9140636.
- [21] P. Livreri, F. Beccaccio, "Optical Plasmonic Nanoantenna-MWCNT diode Energy Harvester for Solar Powered Wireless Sensors", 2021 IEEE Sensors Conference, 2021, pp. 1-4, doi: 10.1109/SENSORS47087.2021.963975
- [22] R. Citroni, F.Di Paolo, P. Livreri, "Evaluation of an Optical Energy Harvester for SHM Applications", *AEU - International Journal of Electronics and Communications* Volume 111, November 2019, 152918
- [23] R. Citroni, F. Di Paolo, P. Livreri, "A Novel Energy Harvester for Powering Small UAVs: Performance Analysis, Model Validation and Flight Results", *Sensors* (2019).
- [24] Gadalla, M. N., Abdel-Rahman, M. & Shamim, A. Design, optimization and fabrication of a 28.3 thz nano-rectenna for infrared detection and rectification. *Scientific Reports* 4, 4270 (2014).
- [25] G. Raimondi, R. Badalamenti, P. Livreri, "Trade-off Performance of Optical Nanoantennas for Solar Energy Harvesting Applications", 2019 SBMO/IEEE MTT-S International Microwave and Optoelectronics Conference (IMOC) , 2019, pp. 1-3 , doi: 10.1109/IMOC43827.2019.9317426.
- [26] Do T.Nga, Do C.Nghia, Chu V.Ha (2017), "Plasmonic properties of graphene-based nanostructures in terahertz waves".
- [27] Shaloo Rakheja, Parijat Sengupta, and Suhaila M. Shakiah (2020), "Design and Circuit Modeling of Graphene Plasmonic Nanoantennas".
- [28] De Fazio, D., Purdie, D.G., Ott, A.K., Braeuninger-Weimer, P., Khodkov, T., Goossens, S., Taniguchi, T., Watanabe, K., Livreri, P., Koppens, F.H.L., Hofmann, S., Goykhman, I., Ferrari, A.C., Lombardo, A., High-Mobility, Wet-Transferred Graphene Grown by Chemical Vapor Deposition. *ACS Nano*, Vol. 13, Issue 8, (2019).
- [29] R. Citroni, F. Di Paolo, P. Livreri, "Progress in THz Rectifier Technology: Research and Perspectives", *Nanomaterials* 12 (14), 2022.
- [30] Hwan Lee, S.; Sup Choi, M.; Lee, J.; Ho Ra, C.; Liu, X.; Hwang, E.; Hee Choi, J.; Zhong, J.; Chen, W.; Jong Yoo, W. High performance vertical tunneling diodes using graphene/hexagonal boron nitride/graphene hetero-structure. *Appl. Phys. Lett.* **2014**, 104, 053103.
- [31] P. Livreri, "A 3.3 V Output Voltage Optical Plasmonic Solar Energy Harvester", 2021 10th International Conference on Renewable Energy Research and Application (ICRERA), 2021, pp. 310-313, doi: 10.1109/ICRERA52334.2021.9598592.